Measurement of the branching ratios $\psi' \rightarrow e^+ e^-$, $\psi' \rightarrow J/\psi \pi \pi$, and $\psi' \rightarrow J/\psi \eta$

T. A. Armstrong,[6] D. Bettoni,[2] V. Bharadwaj,[1] C. Biino,[7] G. Borreani,[7] D. Broemmelsiek,[5] A. Buzzo,[3] R. Calabrese,[2]
A. Ceccucci,[7] R. Cester,[7] M. Church,[1] P. Dalpiaz,[2] P. F. Dalpiaz,[2] D. Dimitroyannis,[5] M. Fabbri,[2] J. Fast,[4]
A. Gianoli,[2] C. M. Ginsburg,[5] K. Gollwitzer,[4] G. Govi,[7] A. Hahn,[1] M. Hasan,[6] S. Hsueh,[1] R. Lewis,[6] E. Luppi,[2]
M. Macrí,[3] A. M. Majewska,[6] M. Mandelkern,[4] F. Marchetto,[7] M. Marinelli,[3] J. Marques,[5] W. Marsh,[1]
M. Martini,[2] M. Masuzawa,[5] E. Menichetti,[7] A. Migliori,[7] R. Mussa,[7] S. Palestini,[7]
M. Pallavicini,[3] S. Passaggio,[3] N. Pastrone,[7] C. Patrignani,[3] J. Peoples, Jr.,[1,5] F. Petrucci,[2] M. G. Pia,[3] S. Pordes,[1]
P. Rapidis,[1] R. Ray,[5,1] J. Reid,[6] G. Rinaudo,[7] E. Robutti,[3] B. Roccuzzo,[7] J. Rosen,[5] A. Santroni,[3] M. Sarmiento,[5]
M. Savrie,[2] J. Schultz,[4] K. K. Seth,[5] A. J. Smith,[4] G. A. Smith,[6] M. Sozzi,[7]
S. Trokenheim,[5] M. F. Weber,[4] S. Werkema,[1] Y. Zhang,[6] J. Zhao,[5] and G. Zioulas[4]

(Fermilab E760 Collaboration)

[1]*Fermi National Accelerator Laboratory, Batavia, Illinois 60510*
[2]*Instituto Nazionale di Fisica Nucleare and University of Ferrara, 44100 Ferrara, Italy*
[3]*Instituto Nazionale di Fisica Nucleare and University of Genoa, 16146 Genoa, Italy*
[4]*University of California at Irvine, California 92717*
[5]*Northwestern University, Evanston, Illinois 60208*
[6]*Pennsylvania State University, University Park, Pennsylvania 16802*
[7]*Instituto Nazionale di Fisica Nucleare and University of Turin, 10125 Turin, Italy*

We have observed exclusive decays of the ψ' in an experiment where the ψ' is formed in antiproton-proton annihilations. We report the branching ratios $B(\psi' \rightarrow e^+ e^-) = (8.3 \pm 0.5_{\text{stat}} \pm 0.7_{\text{syst}}) \times 10^{-3}$, $B(\psi' \rightarrow J/\psi \pi^+ \pi^-) = 0.283 \pm 0.021_{\text{stat}} \pm 0.020_{\text{syst}}$, $B(\psi' \rightarrow J/\psi \pi^0 \pi^0) = 0.184 \pm 0.019_{\text{stat}} \pm 0.013_{\text{syst}}$, $B(\psi' \rightarrow J/\psi \eta) = 0.032 \pm 0.010_{\text{stat}} \pm 0.002_{\text{syst}}$. [S0556-2821(97)04403-2]

PACS number(s): 13.75.Cs, 14.40.Gx

I. INTRODUCTION

Exclusive decays of the ψ' have been observed in formation in a number of $e^+ e^-$ annihilation experiments, notably Mark I and DASP [1]. In certain of the decay modes, such as $\psi' \rightarrow$ leptons, there are large backgrounds from quantum electrodynamic (QED) processes in these experiments. In other modes containing final state γ's, the accuracy of fitting specific hypotheses is limited by the electromagnetic calorimetry of the $e^+ e^-$ collider general purpose detectors.

Fermilab experiment E760 is devoted to high resolution studies of charmonium formed in antiproton-proton annihilation and is described elsewhere [2]. It is designed to observe charmonium decay to final states containing electrons and γ rays. In decays in which high mass $e^+ e^-$ pairs are observed, the backgrounds are extremely small, allowing accurate determinations of branching ratios. The experiment is located at the Antiproton Source where the circulating antiproton beam intersects an internal H$_2$ gas jet target.

II. METHOD

We have collected a low background sample of ψ' events observed in the processes:

$$\bar{p}p \rightarrow \psi' \rightarrow e^+ e^-, \qquad (1)$$

$$\bar{p}p \rightarrow \psi' \rightarrow J/\psi + X \rightarrow e^+ e^- + X. \qquad (2)$$

The inclusive reaction includes, but is not limited to, the specifically identified final states $J/\psi \pi^0 \pi^0$, $J/\psi \pi^+ \pi^-$, and $J/\psi \eta$.

By measuring the ratio of the number of events collected for a specific ψ' decay channel to the number collected for the $J/\psi X$ channel, for which the branching ratio is well measured in $e^+ e^-$ annihilations, we are able to make a better than world average measurement of $B(\psi' \rightarrow e^+ e^-)$ and measurements of $B(\psi' \rightarrow J/\psi \pi^0 \pi^0)$ and $B(\psi' \rightarrow J/\psi \pi^+ \pi^-)$ with errors comparable to the world average. We also determine $B(\psi' \rightarrow J/\psi \eta)$, which is, however, better measured by other experiments.

In order to determine $B(\psi' \rightarrow e^+ e^-)$, we use previous results for $B(\psi' \rightarrow J/\psi X)$ and $B(J/\psi \rightarrow e^+ e^-)$. The world average for $B(J/\psi \rightarrow e^+ e^-)$ is $(5.99 \pm 0.25) \times 10^{-2}$ and that for $B(\psi' \rightarrow J/\psi X)$ is 0.57 ± 0.04 [3]. Together, these two measurements contribute a limiting 8% systematic error to our results. The expression for the branching fraction of ψ' to $e^+ e^-$ is

$$B(\psi' \rightarrow e^+ e^-)$$

$$= \frac{\epsilon_{J/\psi X}}{\epsilon_{ee}} \frac{N_{ee}}{N_{J/\psi X}} B(\psi' \rightarrow J/\psi X) B(J/\psi \rightarrow e^+ e^-). \quad (3)$$

In this equation, ϵ_{ee} and $\epsilon_{J/\psi X}$ include the geometrical acceptance and efficiencies for triggering and selection of the exclusive ($e^+ e^-$) and inclusive ($J/\psi X$ with $J/\psi \rightarrow e^+ e^-$) decays of ψ', respectively. N_{ee} and $N_{J/\psi X}$ are the numbers of exclusive and inclusive events selected, respectively.

TABLE I. ψ' and background running conditions.

Resonance	$E_{c.m.}$ (MeV)	$\int \mathcal{L} dt$ (nb^{-1})
ψ' (1990)	3685–3687	1494
ψ' background (1990)	3655	184
ψ' (1991)	3685–3687	995
ψ' background (1991)	3667	299

Similarly, the expression for the ψ' branching fraction to final state f, where f is $J/\psi\,\pi^0\pi^0$, $J/\psi\,\pi^+\pi^-$, or $J/\psi\,\eta$ is

$$B(\psi' \to f) = \frac{\epsilon_{J/\psi X}}{\epsilon_f} \frac{N_f}{N_{J/\psi X}} B(\psi' \to J/\psi X). \quad (4)$$

π^0 and η are detected through their decays to $\gamma\gamma$ and $\gamma e^+ e^-$ and the respective branching fractions are included in the efficiencies. Here, the limiting systematic error contributed by the measurement of $B(\psi' \to J/\psi X)$ is 7%.

This measurement is based on 2489 nb^{-1} of data taken in two separate running periods in 1990 and 1991 at the formation energy of the ψ', in which 3039 candidates for $\psi' \to e^+ e^-(X)$ were recorded, yielding 2491 selected events. 483 nb^{-1} of data were taken at nearby energies to determine backgrounds. Table I summarizes these data.

III. EXPERIMENTAL APPARATUS

The circulating antiproton beam ($\leqslant 4 \times 10^{11} \bar{p}$) intersects an internal H$_2$ gas jet target ($\leqslant 10^{14}$atoms/cm^2) installed in one of the low dispersion sections of the accumulator ring, giving a peak luminosity of up to 1.0×10^{31}cm^{-2}sec^{-1}.

The central E760 detector has cylindrical symmetry and is depicted in Fig. 1. The elements of the detector which are important for these measurements are the threshold Čerenkov detector [4] which provides electron identification and covers the full azimuthal angular range and the polar angular range from 15° to 70°; the lead glass central calorimeter (CCAL) [5] which covers the full azimuthal range and the polar angular range 11° to 70°; and the inner tracking chamber, a radial projection chamber (RPC) [6], which covers the full azimuth, the polar angular range 15° to 70°, and provides tracking and dE/dx information. The lead-scintillator sandwich forward calorimeter (FCAL) [7] covers the polar angular range 2° to 12°. Additional tracking is provided by cylindrical and forward straw tube chambers, a cylindrical multiwire proportional chamber (MWPC) integrated with the
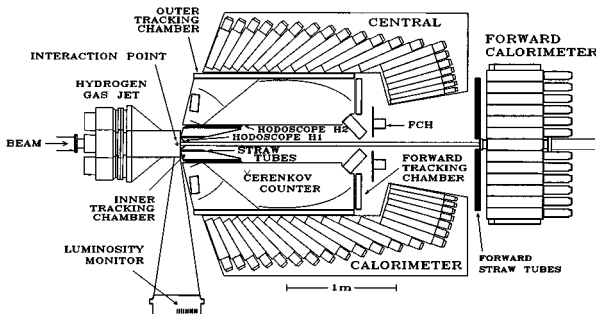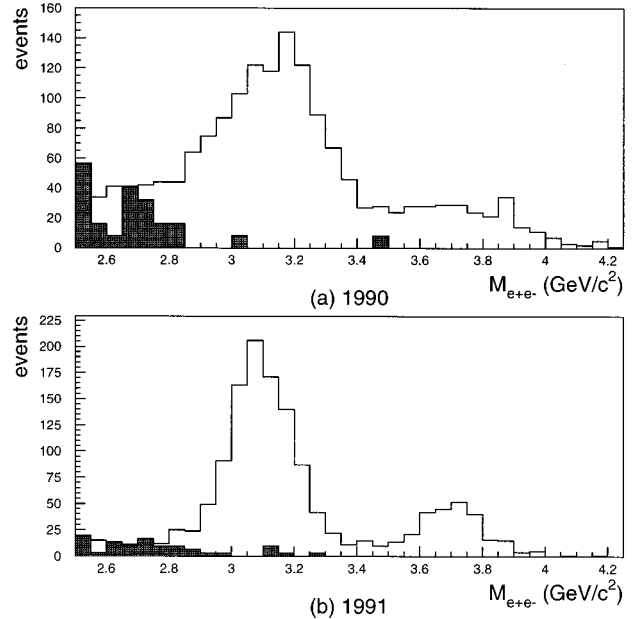

FIG. 2. e^+e^--invariant mass of ψ' candidate events for (a) 1990 and (b) 1991 running.

RPC, the outer tracking chamber consisting of two layers of limited streamer tubes, and the forward tracking chamber, a planar MWPC.

For electromagnetic showers of electrons and γ's, CCAL gives an average resolution of $\sigma_E/E = 0.014 + 0.06/\sqrt{E(\text{GeV})}$ for the energy, 6 Mrad for σ_θ and 12 Mrad for σ_ϕ, where the angular errors include the uncertainty in the annihilation location. CCAL is not instrumented with time to digital converters (TDCs). However, for the 1991 data, nearly all showers with energies above 150 MeV can be identified as "in time" or "out of time" by means of a system of analogue to digital converters (ADCs) with overlapping gates, described in Ref. [8]. In this analysis, we utilize timing information for showers with energies greater than 200 MeV. Showers with smaller energies are identified as "undetermined." The energy resolution of FCAL for γ's and electrons is $\sigma_E/E = 0.19/\sqrt{E(\text{GeV})}$. Its spatial resolution at the face of the detector is $\sigma_x = \sigma_y = 3$ cm. For this analysis, the FCAL threshold is taken as 200 MeV. Charged particle tracking is characterized by an average angular resolution of 4 Mrad in θ and 7 Mrad in ϕ.

Two cylindrical plastic scintillator hodoscopes (H1 and H2) are used for triggering. The pulse heights in H2, together with those in the Čerenkov detector, are used to distinguish singly charged particles from electron-positron pairs due to γ conversions and Dalitz decays.

IV. TRIGGER AND EVENT SELECTION

The hardware trigger used to obtain these data required a pattern of hits in the cylindrical hodoscopes and the Čerenkov counter consistent with two electrons originating at the beam target intersection point. At least two Čerenkov hits were required. Up to four hits in each hodoscope were allowed in order to trigger on the $J/\psi\,\pi^+\pi^-$ channel. The trigger independently required two high-energy showers in

FIG. 1. E760 detector layout.

TABLE II. 1990 ψ' data.

Data set	Candidates	e^+e^- (4C)	$J/\psi X$ (1C)	$J/\psi \pi^+\pi^-$	$J/\psi \pi^0\pi^0$ (7C)	$J/\psi \eta$ (6C)
ψ' data	1643	216	1029	217	87	23
Background	25	0	2	5	0	0
Effective back.	203 ± 41	0 ± 8	16 ± 11	41 ± 18	0 ± 8	0 ± 8
Internal back.		0	15	1	0	1.5
Signal		216 ± 17	998 ± 34	175 ± 23	87 ± 12	21.5 ± 9

CCAL which were separated by more than 90°. Each of these showers was required to be loosely consistent with the kinematics of $J/\psi \to e^+e^-$ decay. This condition accepted events with e^+e^- effective mass greater than about 2.2 GeV/c^2 with full efficiency.

The trigger places no charge requirement on additional showers accompanying the electron candidates. Showers due to e^+e^- (Dalitz) pairs are thus treated identically to those produced by γ's. π^0 and η decays to $e^+e^-\gamma$ and $e^+e^-e^+e^-$ are included in our event sample.

The hodoscope hits, Čerenkov signals, and calorimeter showers are associated off line into tracks. The two electron candidates are identified as the tracks with the largest two-body effective mass.

The charged multiplicity requirement is the only trigger element which may differ in efficiency among these ψ' decay channels. This is because of extra hits in the H1 and H2 hodoscopes which can raise the H1 or H2 multiplicity above four, decreasing the efficiency, especially for the $J/\psi \pi^+\pi^-$ channel. The extra hits in H1 are mainly δ rays from the target and the rate for these is determined from $\psi' \to e^+e^-$ events. The extra hits in H2 are mainly δ rays from interactions of charged tracks in the detector. This rate is found to be consistent with the detector material inventory. The effects of the multiplicity requirement and the other trigger conditions are included in the simulation [9] used to calculate efficiencies.

The data taken in the 1990 and 1991 runs are analyzed separately. The charged track definition in the trigger was different in the two runs; a slightly wider angular window in the H1-H2 coincidence was used in 1991 to increase the trigger efficiency. In 1990 we calibrated CCAL using 4000 $J/\psi \to e^+e^-$ events which did not fully sample the calorimeter, in conjunction with previously obtained bench measurements. In 1991 we calibrated the entire calorimeter *in situ* using a large sample of $\bar{p}p \to \pi^0\pi^0$ events. Another significant difference is that much less background data was taken in 1990.

In this analysis the cuts are relatively loose and data collected near the ψ' resonance under the same running conditions are used to estimate backgrounds. The following cuts are applied to select ψ' decay candidates: $\theta_{e^+}^{\text{lab}}$ and $\theta_{e^-}^{\text{lab}} \in [15°,60°]$; $M_{e^+e^-} > 2.5$ GeV/c^2; $(\text{ELW}_{e^+} \times \text{ELW}_{e^-}) > \text{ELWCUT}$.

The electron weight index (ELW) [9] is constructed for each electron candidate from pulse heights in the H2 and Čerenkov counters, dE/dx from the RPC, second moments of the transverse shower distribution in CCAL, and the fractional shower energy in a 3x3 block region of CCAL. ELW is a likelihood ratio for the electron hypothesis versus the background track hypothesis.

In Fig. 2 we give histograms of the e^+e^--invariant mass for the candidate events for the 1990 and 1991 data separately. The shaded histograms are obtained by making the same selection for off-resonance background running and are normalized by integrated luminosity.

Backgrounds are further reduced by the following kinematical and topological selection criteria.

$\psi' \to e^+e^-$ events are selected using a four constraint (4C) kinematical fit. All candidate events are tested with this and the 1C $J/\psi X$ hypothesis. Because estimated uncertainties for energies and angles in the calorimeter are not normally distributed, and off-diagonal errors for the measurements are not estimated, χ^2 cannot be translated into an accurate fit probability, requiring that the fit efficiencies be determined by Monte Carlo simulation.

Inclusive $\psi' \to J/\psi X$ decays are selected using a 1C kinematical fit where M_X is unconstrained. Because this fit is weakly constrained, the additional requirement that the nominal fit probability for the hypothesis $\psi' \to e^+e^-$ is less that 10^{-6} is also applied.

ψ' decays to $J/\psi \pi^0\pi^0 \to e^+e^-\gamma\gamma\gamma\gamma$ and $J/\psi \eta \to e^+e^-\gamma\gamma$ are selected by means of 7C and 6C kinematical fits, respectively. For 1990 data all candidate events with at least 4(2) CCAL and/or FCAL showers apart from

TABLE III. 1991 ψ' data.

Data set	Candidates	e^+e^- (4C)	$J/\psi X$ (1C)	$J/\psi \pi^+\pi^-$	$J/\psi \pi^0\pi^0$ (7C)	$J/\psi \eta$ (6C)
ψ' data	1396	248	993	199	70	17
Background	34	0	10	3	0	0
Effective back.	114 ± 19	0 ± 3	33 ± 11	10 ± 6	$\ll1$	0 ± 3
Internal back.		0	7	1	0	2
Signal		248 ± 16	953 ± 33	188 ± 15	70 ± 9	15 ± 5

TABLE IV. Trigger efficiencies for ψ' decay channels.

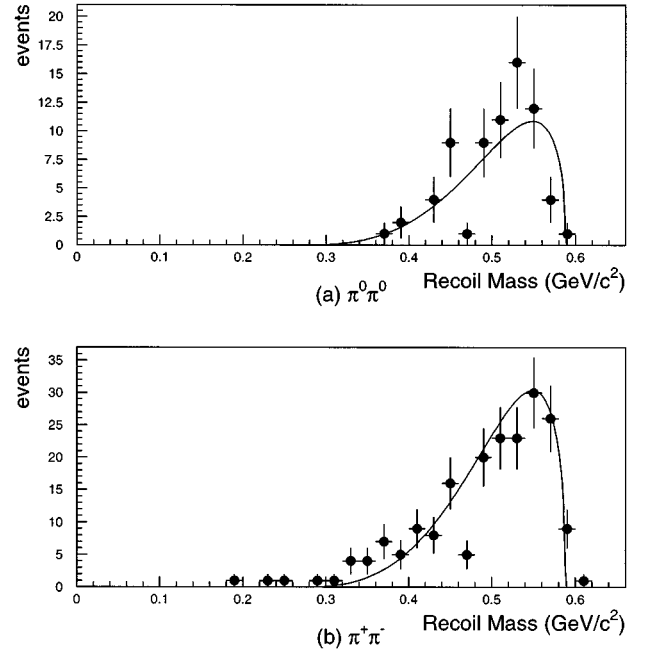| Channel	$\left(\dfrac{\epsilon_{J/\psi X}}{\epsilon_f}\right)_{\mathrm{trig}}$ (1990)	$\left(\dfrac{\epsilon_{J/\psi X}}{\epsilon_f}\right)_{\mathrm{trig}}$ (1991)
$\psi' \to e^+ e^-$	0.903 ± 0.005	0.900 ± 0.005
$\psi' \to J/\psi\,\pi^+\pi^-$	1.070 ± 0.005	1.070 ± 0.005
$\psi' \to J/\psi\,\pi^0\pi^0$	0.952 ± 0.009	0.944 ± 0.009
$\psi' \to J/\psi\,\eta$	0.808 ± 0.041	0.802 ± 0.041

the electron showers are tested with the $J/\psi\,\pi^0\pi^0$ ($J/\psi\,\eta$) hypothesis. For 1991 data only in-time and undetermined showers are considered and the former must be included in the fit.

ψ' decays to $J/\psi\,\pi^+\pi^-$ are selected by topological cuts alone. $J/\psi\,\pi^+\pi^-$ candidates are required to have four nonadjacent hits in the H2 hodoscope and may have any number of calorimeter showers. The two hodoscope hits not associated with electron tracks are required to be unassociated with Čerenkov counter hits beyond those due to the electron tracks. This Čerenkov counter requirement is made to exclude backgrounds from the $J/\psi\,\pi^0\pi^0$ channel where a γ from π^0 decay converts or a π^0 Dalitz decays to $e^+e^-\gamma$.

Tables II and III give the selected event totals for 1990 and 1991, respectively, for the ψ' and background samples. The effective background reported is the measured background normalized for integrated luminosity. For the $\psi' \to e^+e^-$ channel it includes the continuum $\bar{p}p \to e^+e^-$ channel which contributes approximately one event. We observe that the luminosity normalized background is roughly the same in 1991 as in 1990, while the ψ' rate is larger in 1991. This is a consequence of our taking a greater fraction of the data close to the ψ' peak in 1991. The internal background is the expected number of events from real ψ' decays to other channels that are misidentified, as determined by our simulation. Systematic errors on internal backgrounds are insignificant in this analysis. The simulation includes $\psi' \to J/\psi\,\pi^+\pi^-$, $\psi' \to J/\psi\,\pi^0\pi^0$, $\psi' \to J/\psi\,\eta$, and ψ' radiative transitions through the χ states. We include radiative decays of the J/ψ and ψ' to $e^+e^-\gamma$ as predicted by QED [10]. Neglect of these radiative modes would lead to an overestimation of the 4C fit efficiency by about 5% and the 1C fit efficiency by about 1%. In the 1991 data, the effective background for the decay to $J/\psi\,\pi^0\pi^0$ is determined to be much smaller than one event from studies of a large data sample (6 pb^{-1}) collected in the search for the η'_c in the vicinity of 3.6 GeV/c^2 [11].

FIG. 3. Mass recoiling against J/ψ for (a) $J/\psi\,\pi^0\pi^0$ and (b) $J/\psi\,\pi^+\pi^-$ decays of ψ'.

V. EFFICIENCIES

The crucial element in this analysis is an accurate determination of the relative efficiency for each individual exclusive decay to the inclusive decay $J/\psi X$. The efficiency for each decay channel is the product of its trigger efficiency and the efficiencies for the electron weight cut, the e^+e^- mass cut, and for kinematical fitting or topological selection.

A. Trigger efficiency

The Monte Carlo simulation determines the trigger efficiency for each channel, which includes the geometric acceptance for the e^+ and e^-. By studying $J/\psi \to e^+e^-$ decays, we find that the Čerenkov efficiency was uniform over the angular region $15° < \theta < 60°$, with the exception of the region $33° < \theta < 39°$, corresponding to the septa which divide each (of 8) Čerenkov cell into two gas volumes. The simulation models the reduced efficiency in that region. The possible systematic effect of the Čerenkov trigger efficiency parametrization is studied by excluding events with one or two electrons in that angular region, and is found to be negligible.

TABLE V. Measured and simulated selection efficiencies for ψ' decays and other decay channels.

Channel	ϵ_{sel} MC (1990)	ϵ_{sel} MC (1991)	ϵ_{sel} Meas. (1991)
$\psi' \to e^+e^-$	0.715 ± 0.047	0.848 ± 0.01	
$\psi' \to J/\psi X$	0.853 ± 0.024	0.932 ± 0.01	
$\psi' \to J/\psi\,\pi^+\pi^-$	0.369	0.368	
$\psi' \to J/\psi\,\pi^0\pi^0$	0.188 ± 0.009	0.224 ± 0.014	
$\psi' \to J/\psi\,\eta$	0.488 ± 0.022	0.546 ± 0.017	
$J/\psi \to e^+e^-$		0.896 ± 0.005	0.894 ± 0.005
$\chi_2 \to e^+e^-\gamma$		0.902 ± 0.007	0.916 ± 0.006

TABLE VI. Efficiencies, selected event totals, and branching fractions for the ψ' final states.

Channel		$\dfrac{\epsilon_{J/\psi X}}{\epsilon_f}$	$\dfrac{N_f}{N_{J/\psi X}}$	B
$\psi' \to e^+ e^-$	1990	1.061 ± 0.037	0.216 ± 0.019	$(7.8 \pm 0.7_{\text{stat}} \pm 0.6_{\text{syst}}) \times 10^{-3}$
	1991	0.981 ± 0.013	0.260 ± 0.019	$(8.7 \pm 0.7_{\text{stat}} \pm 0.7_{\text{syst}}) \times 10^{-3}$
$\psi' \to J/\psi \, \pi^+ \pi^-$	1990	2.46 ± 0.08	0.175 ± 0.024	$0.247 \pm 0.036_{\text{stat}} \pm 0.018_{\text{syst}}$
	1991	2.71 ± 0.035	0.197 ± 0.017	$0.304 \pm 0.027_{\text{stat}} \pm 0.021_{\text{syst}}$
$\psi' \to J/\psi \, \pi^0 \pi^0$	1990	4.32 ± 0.35	0.087 ± 0.012	$0.214 \pm 0.035_{\text{stat}} \pm 0.015_{\text{syst}}$
	1991	3.93 ± 0.27	0.073 ± 0.009	$0.165 \pm 0.024_{\text{stat}} \pm 0.012_{\text{syst}}$
$\psi' \to J/\psi \, \eta$	1990	3.64 ± 0.22	0.022 ± 0.009	$0.046 \pm 0.019_{\text{stat}} \pm 0.003_{\text{syst}}$
	1991	3.53 ± 0.20	0.016 ± 0.005	$0.032 \pm 0.010_{\text{stat}} \pm 0.002_{\text{syst}}$

The efficiencies are sensitive to the rate of spurious counts in the H1 and H2 hodoscope arrays and to the angular distribution of the e^+ and e^-. The trigger contains the multiplicity cuts: $N_{H1} \leq 4$ and $N_{H2} \leq 4$, which have the effect that $\psi' \to J/\psi \, \pi^+ \pi^-$ events are rejected in the case of a spurious hit in either hodoscope.

The decays to $J/\psi \, \pi^+ \pi^-$ and $J/\psi \, \pi^0 \pi^0$ are characterized by an S-wave decay to J/ψ and a $J^P = 0^+$ $\pi\pi$ system [12]. The angular distribution of the J/ψ is isotropic and the $e^- (e^+)$ angular distribution is the same as that of the $e^+ e^-$ exclusive decay, albeit in the J/ψ rather than the ψ' frame. The $e^- (e^+)$ angular distribution for all of these modes is $1 + \lambda_{\psi'} \cos^2 \theta^*$, where $\lambda_{\psi'}$ is determined by $\bar{p} p \to \psi'$ formation amplitudes and $\cos \theta^*$ is the electron polar angle in the ψ' (for $e^+ e^-$) or J/ψ frame. The $J/\psi \pi\pi$ decay is about 90% of the $J/\psi X$ inclusive decay which thus has nearly the same $e^- (e^+)$ angular distribution as the $e^+ e^-$ exclusive decay. Using this constraint, we find that the ratio of $J/\psi X$ to $e^+ e^-$ acceptance varies by only 0.5% over a wide range of allowed values for $\lambda_{\psi'}$. This is despite the fact that the absolute acceptances for these reactions vary by more than 10% over the same range of $\lambda_{\psi'}$. We take $\lambda_{\psi'} = 0.69 \pm 0.26$, the value previously reported by this experiment [2]. For the decay to $J/\psi \, \eta$, the angular distribution of the J/ψ is anisotropic and given by $1 + \lambda_{\psi'} \cos^2 \theta$ (θ is the J/ψ polar angle in the ψ' frame) and the angular distribution of the $e^- (e^+)$ in the J/ψ frame is given by $(1 + 5\lambda_{\psi'}/4 - \lambda_{\psi'} \cos^2 \theta^*)$ [9]. Table IV gives the ratios of the inclusive decay trigger efficiency to those for the exclusive decays.

B. Electron weight and mass cut efficiencies

The efficiency of the electron weight cut is determined experimentally by applying it to a clean sample of $\bar{p} p \to J/\psi \to e^+ e^-$ selected by a kinematical fit. For the 1990 (1991) J/ψ data, this cut has an efficiency of 0.974 ± 0.004 (0.983 ± 0.002). The efficiency of the electron weight cut for the ψ' channels is high and nearly channel independent. It does not affect $\epsilon_{J/\psi X}/\epsilon_f$.

The efficiency of the $e^+ e^-$ mass cut is smaller for $J/\psi X \to e^+ e^- X$ decays of the ψ' than for the higher mass $\psi' \to e^+ e^-$ decays. Using the GEANT simulation [13], the ratio of efficiencies for the mass cut for the 1990 (1991) data is determined to be $[(\epsilon_{J/\psi X})/\epsilon_{ee}]_{M_{ee}} = 0.985 \pm 0.003 (0.992 \pm 0.004)$.

C. Selection efficiency

The efficiencies for event selection are determined by the simulation. Table V gives the calculated selection efficiency for each of the ψ' decay channels for both 1990 and 1991 conditions. Modeling of the uncertainties used in kinematical fitting dominates the quoted errors with the exception of the $J/\psi \, \pi^+ \pi^-$ channel where the efficiency for topological selection is entirely geometrical. The selection efficiencies for $J/\psi \, \pi^0 \pi^0$ and $J/\psi \, \eta$ include the geometrical acceptances for the π^0 and η decay γ's, which, as they are not required in the trigger, are not included in the respective trigger efficiencies. The selection efficiency for $J/\psi \, \pi^+ \pi^-$ similarly includes the geometrical acceptance for the π^+ and π^-. The table includes calculated and measured efficiencies for fits to

TABLE VII. Comparison of E760 results for ψ' branching fractions with previous determinations.

Channel	E760	Previous	Ref.
$\psi' \to e^+ e^-$	$(8.3 \pm 0.5_{\text{stat}} \pm 0.7_{\text{syst}}) \times 10^{-3}$	$(9.3 \pm 1.6) \times 10^{-3}$	Mark I [14]
		$(8.8 \pm 1.3) \times 10^{-3}$	PDG [3]
$\psi' \to J/\psi \, \pi^+ \pi^-$	$0.283 \pm 0.021_{\text{stat}} \pm 0.020_{\text{syst}}$	0.32 ± 0.04	Mark I [15]
		0.36 ± 0.06	DASP [16]
		0.324 ± 0.026	PDG [3]
$\psi' \to J/\psi \, \pi^0 \pi^0$	$0.184 \pm 0.019_{\text{stat}} \pm 0.013_{\text{syst}}$	0.18 ± 0.06	DASP [16]
		0.184 ± 0.027	PDG [3]
$\psi' \to J/\psi \, \eta$	$0.032 \pm 0.010_{\text{stat}} \pm 0.002_{\text{syst}}$	0.025 ± 0.006	Mark II [17]
		0.0218 ± 0.0038	CBAL [18]
		0.036 ± 0.005	CNTR [19]
		0.027 ± 0.004	PDG [3]

$\bar{p}p \rightarrow J/\psi \rightarrow e^+e^-$ and $\bar{p}p \rightarrow \chi_2 \rightarrow J/\psi \gamma \rightarrow e^+e^-\gamma$. J/ψ and χ_2 events can be cleanly selected with only electron weight and mass cuts, making it possible to measure their selection efficiencies directly. The J/ψ events are selected by a 4C fit, and the χ_2 sample by a 1C fit to $J/\psi X$ where the γ is not used and M_X is unconstrained. The Monte Carlo (MC) simulation agrees well with these measured selection efficiencies.

D. Overall efficiencies and ψ' branching fractions

In Table VI we give the ratio of events selected for each exclusive decay to events selected for $J/\psi X$. The ratios of overall efficiencies, which include trigger, selection, and the e^+e^- mass cut are given, as are the branching fractions computed using expressions 3 and 4. Systematic errors are obtained from uncertainties in $\psi' \rightarrow J/\psi X$ and $J/\psi \rightarrow e^+e^-$ branching ratios and in detector acceptances.

VI. RESULTS

We combine the 1990 and 1991 results to obtain the best estimates of the branching fractions, which are given in Table VII with previously published values and the Particle Data Group (PDG) [3] world averages. Statistical errors are added in quadrature and systematic errors are carried through each average unchanged. We observe that our results are consistent with previous determinations and significantly improve upon the world average for the $\psi' \rightarrow e^+e^-$ mode. They modestly improve upon the world average for the $\psi' \rightarrow J/\psi \pi^+\pi^-$ and $\psi' \rightarrow J/\psi \pi^0\pi^0$ modes. In Fig. 3 we give the $\pi\pi$ effective mass distributions for events selected as $\psi' \rightarrow J/\psi \pi^+\pi^-$ and $\psi' \rightarrow J/\psi \pi^0\pi^0$. The data is consistent with the predictions of Ref. [12], based on the S-wave decay of ψ' to an S-wave $\pi\pi$ system with final state interactions.

[1] R. Brandelik *et al.*, Z. Phys. C **1**, 233 (1979); W. Tanenbaum *et al.*, Phys. Rev. D **17**, 1731 (1978).

[2] T. Armstrong *et al.*, Phys. Rev. D **47**, 772 (1993).

[3] Particle Data Group, R. D. Barnett *et al.*, Phys. Rev. D **54**, 1 (1996).

[4] C. Biino *et al.*, Nucl. Instrum. Methods Phys. Res. A **317**, 135 (1992).

[5] L. Bartoszek *et al.*, Nucl. Instrum. Methods Phys. Res. A **301**, 47 (1991).

[6] R. Calabrese *et al.*, Nucl. Instrum. Methods Phys. Res. A **277**, 116 (1989).

[7] M. A. Hasan *et al.*, Nucl. Instrum. Methods Phys. Res. A **295**, 73 (1990).

[8] K. E. Gollwitzer, Ph.D. thesis, University of California, Irvine, 1993.

[9] A. J. Smith, Ph.D. thesis, University of California, Irvine, 1993.

[10] T. Armstrong *et al.*, Phys. Rev. D **54**, 7067 (1996).

[11] T. Armstrong *et al.*, Phys. Rev. D **52**, 4839 (1995).

[12] T. N. Pham *et al.*, Phys. Lett. **61B**, 183 (1976).

[13] ''GEANT Detector Description and Simulation Tool,'' CERN Program Library Long Writeup W5013, 1994 (unpublished).

[14] V. Luth *et al.*, Phys. Rev. Lett. **35**, 1124 (1975).

[15] G. Abrams *et al.*, Phys. Rev. Lett. **34**, 1181 (1975).

[16] B. Wiik *et al.*, International Symposium on Lepton-Photon Interactions, Stanford, California, 1995 (unpublished), p. 69.

[17] T. Himel *et al.*, Phys. Rev. Lett. **44**, 920 (1980).

[18] M. Oreglia *et al.*, Phys. Rev. Lett. **45**, 959 (1980).

[19] W. Bartel *et al.*, Phys. Lett. **79B**, 492 (1978).